JNK-Mediated BIM Phosphorylation Potentiates BAX-Dependent Apoptosis

Girish V. Putcha,[1] Siyuan Le,[2] Stephan Frank,[3]
Cagri G. Besirli,[1] Kim Clark,[4] Boyang Chu,[4]
Shari Alix,[4] Richard J. Youle,[3] Art LaMarche,[4]
Anna C. Maroney,[2] and Eugene M. Johnson, Jr.[1],*
[1]Department of Neurology and
Department of Molecular Biology
    and Pharmacology
Washington University School of Medicine
Saint Louis, Missouri 63110
[2]Cephalon Incorporated
West Chester, Pennsylvania 19380
[3]Biochemistry Section
Surgical Neurology Branch
National Institute of Neurological
    Disorders and Stroke
National Institutes of Health
Bethesda, Maryland 20892
[4]Upstate, USA
Lake Placid, New York 12946

Summary

Trophic factor deprivation (TFD) activates c-Jun N-terminal kinases (JNKs), culminating in coordinate AP1-dependent transactivation of the BH3-only BCL-2 proteins BIM_{EL} and HRK, which in turn are critical for BAX-dependent cytochrome c release, caspase activation, and apoptosis. Here, we report that TFD caused not only induction but also phosphorylation of BIM_{EL}. Mitochondrially localized JNKs but not upstream activators, like mixed-lineage kinases (MLKs) or mitogen-activated protein kinase kinases (MKKs), specifically phosphorylated BIM_{EL} at Ser65, potentiating its proapoptotic activity. Inhibition of the JNK pathway attenuated BIM_{EL} expression, prevented BIM_{EL} phosphorylation, and abrogated TFD-induced apoptosis. Conversely, activation of this pathway promoted BIM_{EL} expression and phosphorylation, causing BIM- and BAX-dependent cell death. Thus, JNKs regulate the proapoptotic activity of BIM_{EL} during TFD, both transcriptionally and posttranslationally.

Introduction

Programmed cell death (PCD) culminating in apoptosis is an evolutionarily conserved and genetically regulated process that is critical to normal development and tissue homeostasis. Defects in cell death may contribute to pathologies ranging from oncogenesis and autoimmunity to infertility and neurodegeneration.

In mammals, apoptotic signaling cascades can be divided into two broad categories: the "intrinsic" (i.e., apoptosome) and the "extrinsic" (i.e., death receptor and perforin/granzyme) pathways. As a generalization, intrinsic pathway stimuli require the release of mitochon-

drial proteins, such as cytochrome c (cyt c) and Smac/Diablo, for caspase activation, whereas extrinsic pathway signals usually activate caspases more directly but may engage the mitochondrial pathway for amplification. BCL-2 proteins function at a critical checkpoint in the intrinsic pathway to regulate mitochondrial permeability. Antiapoptotic members (e.g., BCL-2 and BCL-X_L) prevent—and multidomain proapoptotic members (e.g., BAX and BAK) promote—release of mitochondrial apoptogens.

Recognized more recently within the BCL-2 family is a subfamily of proapoptotic molecules that share homology only within the BH3 domain. These "BH3-only" proteins (e.g., BAD, BID, BIM, and HRK) transduce death signals to the mitochondrial checkpoint, culminating in BAX-, BAK-, and/or BOK-dependent release of mitochondrial apoptogens. Regulation of BH3-only proteins is complex and can vary in a cell type- and stimulus-specific manner, as exemplified by BIM, whose proapoptotic activity is modulated at multiple levels: transcriptional, posttranscriptional, and posttranslational.

Transcriptional control of BIM involves contributions from the mixed-lineage kinase (MLK)/c-Jun N-terminal kinase (JNK) (Harris and Johnson, 2001; Putcha et al., 2001; Whitfield et al., 2001), phosphatidylinositol-3-kinase (PI3K)/Akt (Dijkers et al., 2000, 2002), and Ras/mitogen-activated protein kinase (MAPK) pathways (Putcha et al., 2001; Shinjyo et al., 2001) (see Discussion). Furthermore, the observation that expression of BIM_{EL} predominates at the protein level despite coexpression of multiple transcripts (i.e., Bim_{EL}, Bim_L, and Bim_S) potentially suggests a role for posttranscriptional regulation of BIM (Putcha et al., 2001). Finally, in other cell types that express BIM constitutively, its activity is regulated posttranslationally by sequestration to the microtubular dynein motor complex through interaction with DLC1/LC8 (Puthalakath et al., 1999).

Recently, we reported that TFD significantly induces expression of BIM_{EL} genetically upstream of (or in parallel with) the BAX/BCL-2 and caspase checkpoints in multiple neuronal populations in vivo and in vitro, including sympathetic (SCG) and cerebellar granule (CG) neurons (Putcha et al., 2001). Moreover, Bim deficiency delays but does not prevent cyt c release (Putcha et al., 2001) and TFD-mediated neuronal apoptosis (Putcha et al., 2001; Whitfield et al., 2001), suggesting that BIM shares functional redundancy with other BH3-only proteins (e.g., HRK) induced with similar kinetics in these cells (Imaizumi et al., 1997; Harris and Johnson, 2001). In contrast, targeted deletion of other BH3-only proteins (i.e., Bid and Bad) does not alter the kinetics or extent of TFD-induced apoptosis in these paradigms (Putcha et al., 2002). Finally, cell death caused by ectopic overexpression of BH3-only proteins (e.g., BID, BIM, or HRK) requires BAX in CG neurons (Harris and Johnson, 2001; Putcha et al., 2002).

In the course of performing these studies, we observed changes in the migration pattern of BIM_{EL} during TFD. We now report that TFD caused not only induction but also concurrent phosphorylation of BIM_{EL} in SCG

*Correspondence: emjohnson@msnotes.wustl.edu

and CG neurons. Mitochondrially localized JNKs but not their upstream activators MLKs or MKKs phosphorylated BIM_{EL} at Ser65, potentiating its cytotoxicity without altering its subcellular distribution or integration into mitochondrial membranes. Inhibition of the MLK/JNK pathway by either molecular genetic or pharmacological means attenuated BIM_{EL} induction, prevented BIM_{EL} phosphorylation, and abrogated apoptosis caused by TFD. Conversely, activation of this pathway promoted BIM_{EL} expression and phosphorylation, causing cell death that required BAX alone, despite coexpression of BAK. Thus, JNKs regulated BIM_{EL} function during TFD-induced apoptosis at two distinct levels: transcriptional and posttranslational.

Results

Trophic Factor Deprivation Induces MLK/JNK Pathway-Mediated BIM Phosphorylation

TFD in rat SCG or CG neurons caused induction of endogenous BIM_{EL}, which typically migrated as a triplet of $\sim24-26$ kDa when examined by immunoblot analysis in either SCG (Figure 1A) or CG neurons (Figure 1B). (For SCG neurons, these experiments were conducted in the presence of the broad-spectrum caspase inhibitor BAF; for CGNs, the studies were done with neurons from $Bax^{-/-}$ mice. In both cases, these experimental conditions were chosen to allow "early" signaling events genetically upstream of the BAX/BCL-2 and caspase checkpoints to occur, while preventing cell death.) To determine whether these additional bands represented phosphorylated BIM_{EL}, we treated whole-cell lysates from NGF-deprived SCG (Figure 1C) or K^+-deprived CG neurons (Figure 1D) with calf intestine alkaline phosphatase (CIAP). As shown in Figures 1C and 1D, the more slowly migrating bands were eliminated by treatment with CIAP but not by treatment with buffer alone, coincident with a shift to (and increased intensity of) the faster migrating band.

In contrast, CIAP did not alter the band pattern of BCL-2, which migrated as a singlet as seen previously (Putcha et al., 2002), or $BCL-X_L$, which typically migrated as a doublet of ~27 kDa, consistent with amidation of $BCL-X_L$ (Deverman et al., 2002). Furthermore, as additional controls for CIAP activity, we probed for phospho-cJun Ser63 (P-Jun), which increases in intensity with TFD, and phospho-Akt Ser473 (P-Akt), which decreases with TFD. In both SCG and CG neurons, treatment with CIAP but not with buffer alone eliminated phospho-specific antibody immunoreactivity. Taken together with similar findings in mouse SCG and CG neurons, as well as human 293 (data not shown) and SAOS-2 cells (B. Deverman and S. Weintraub, personal communication), these observations indicate that endogenous BIM_{EL} was phosphorylated.

Since our initial report describing BIM induction during neuronal apoptosis (Putcha et al., 2001), we have been examining the contributions of three important signaling modules—MLK/JNK, PI3K/Akt, and Ras/MEK—to BIM transcription (see Discussion). In the process of conducting these studies, we observed that attenuation of MLK/JNK signaling with CEP-1347 (KT7515), an indo-

locarbazole of the K252a family that selectively inhibits MLKs (Maroney et al., 2001), not only decreased BIM_{EL} induction (Harris and Johnson, 2001; Putcha et al., 2001) but also prevented BIM_{EL} phosphorylation in both SCG (Figure 1E) and CG neurons (data not shown). Similarly, the anthrapyrazole JNK inhibitor SP600125 (Bennett et al., 2001; Han et al., 2001) also prevented hyperphosphorylation of BIM_{EL} (Figure 1F). Interestingly, treatment with either CEP-1347 or SP600125 was associated with loss of only the most hyperphosphorylated BIM_{EL} band (Figure 1E, compare lanes 3 and 4; Figure 1F, compare lanes 2 and 3), whereas treatment of extracts with CIAP shifted both hyperphosphorylated BIM_{EL} bands to the hypophosphorylated form (Figure 1E, lanes 2 and 5), consistent with the possibility that kinases other than those of the MLK/JNK pathway may also contribute to BIM_{EL} phosphorylation. In sum, these data indicate that, during TFD in SCG and CG neurons, the MLK/JNK pathway contributes not only to induction but also to phosphorylation of BIM.

Phosphorylation of BIM Potentiates Its Proapoptotic Activity

As described above, TFD caused BIM_{EL} induction and phosphorylation (Figure 1). Moreover, treatment of NGF-deprived SCG or K^+-deprived CG neurons with CEP-1347 or SP600125 partially inhibited BIM_{EL} induction (Harris and Johnson, 2001; Putcha et al., 2001) but completely prevented appearance of the most hyperphosphorylated BIM_{EL} band (Figures 1E and 1F). Finally, CEP-1347 inhibits TFD-induced apoptosis in both SCG (Maroney et al., 1999; Harris et al., 2002a) and CG neurons (Trotter et al., 2002; Harris et al., 2002b). Therefore, we hypothesized that phosphorylation of BIM_{EL} enhances its cytotoxicity.

To test this hypothesis and to identify the phosphorylation site(s) in BIM_{EL}, we performed site-directed mutagenesis, in which certain sites were mutated to Glu or Ala to mimic constitutive phosphorylation and dephosphorylation, respectively. We chose to target three sites conforming to the MAPK consensus sequences S/T-P or P-X-S/T-P for Pro-directed Ser/Thr kinases within the sequence unique to BIM_{EL} (residues 42–97), for several reasons. First, CEP-1347 and SP600125, which inhibit the MLK/JNK pathway (consisting of MAPKs), prevented BIM_{EL} phosphorylation (Figures 1E and 1F). Second, although phosphorylation of BIM_L has been reported, its functional significance remains unclear (Shinjyo et al., 2001), suggesting that phosphorylation sites common to BIM_{EL} and BIM_L may not affect activity. Finally, the three sites (and surrounding consensus sequences) we chose to mutate within the unique BIM_{EL} sequence—Ser55, Ser65, and Ser73—are strictly conserved among humans, rats, and mice (Figures 2A and 2B).

To assess the effects of alanine mutagenesis of these residues on the electrophoretic migration and function of BIM, we first examined lysates from 293 cells transiently transfected with wild-type (wt) Bim_{EL} or various mutants with antibodies to BIM and to the EE epitope tag. Overexpression of Bim_{EL} wt recapitulated the altered migration pattern of endogenous BIM_{EL} seen with TFD in neurons; moreover, CIAP treatment of extracts from 293 cells overexpressing Bim_{EL} wt eliminated hyper-
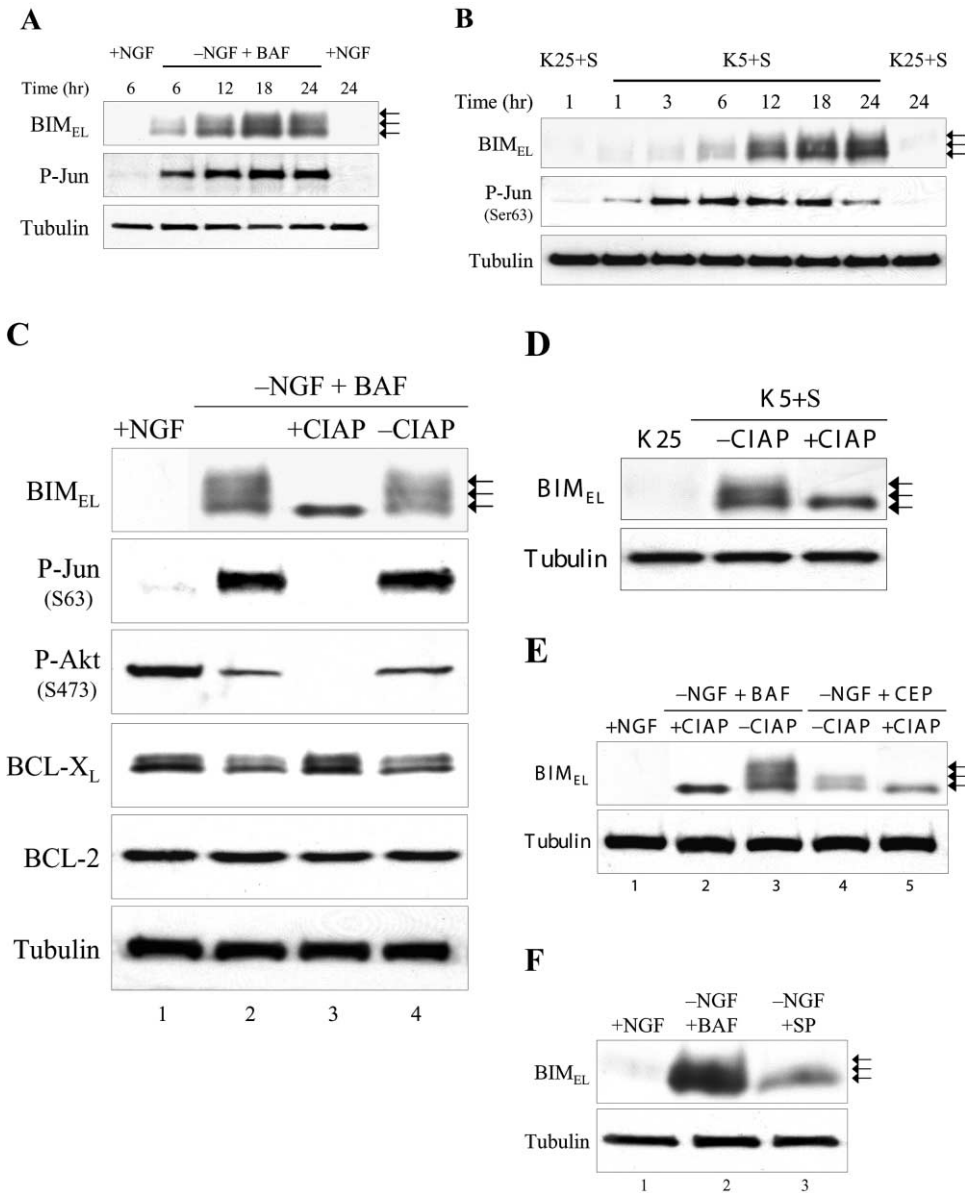
Figure 1. Trophic Factor Deprivation Induces MLK/JNK Pathway-Mediated BIM$_{EL}$ Phosphorylation

(A) SCG neurons (5 days in vitro, DIV5) were maintained in NGF or deprived of NGF in the presence of 50 μM BAF for the indicated times, lysed, and then examined by immunoblotting.

(B) DIV7 *Bax$^{-/-}$* CGNs were maintained in K25 + S or in K5 + S for the indicated times, lysed, and analyzed by Western blotting.

(C) DIV5 SCG neurons were maintained in NGF (lane 1) or deprived of NGF in the presence of 50 μM BAF (lanes 2−4) for 24 hr, lysed, treated with calf intestinal alkaline phosphatase (CIAP) (lane 3) or buffer (lane 4), and examined by immunoblotting.

(D) DIV7 *Bax$^{-/-}$* CGNs were maintained in K25 + S or K5 + S for 24 hr, lysed, treated with CIAP or buffer, and examined by Western blotting.

(E) DIV5 SCG neurons were maintained in NGF (lane 1) or deprived of NGF in the presence of 50 μM BAF (lanes 2 and 3) or 400 nM CEP-1347 (lanes 4 and 5). After 24 hr, whole-cell extracts were prepared, treated with CIAP (lanes 2 and 5) or buffer (lanes 3 and 4), and analyzed by immunoblotting.

(F) DIV5 SCG neurons were maintained in NGF (lane 1) or deprived of NGF in the presence of 50 μM BAF (lane 2) or 14 μM SP600125 (lane 3). After 24 hr, whole-cell extracts were prepared and analyzed by Western blotting.

phosphorylated BIM$_{EL}$ bands (data not shown). Furthermore, sequential S→E mutation of residues 65, 55, and 73 produced progressively slower migrating forms of BIM$_{EL}$ (Figure 2C), and immunoblot analysis of extracts prepared from 293 cells overexpressing any of the S→A mutants demonstrated only hypophosphorylated BIM$_{EL}$

(Figure 2C), suggesting that mutation of the Ser65 site alone might be sufficient to attenuate BIM$_{EL}$ phosphorylation.

We next examined the functional significance of changes in BIM$_{EL}$ phosphorylation in K25 + S-maintained CGNs, a CNS model of activity-dependent sur-
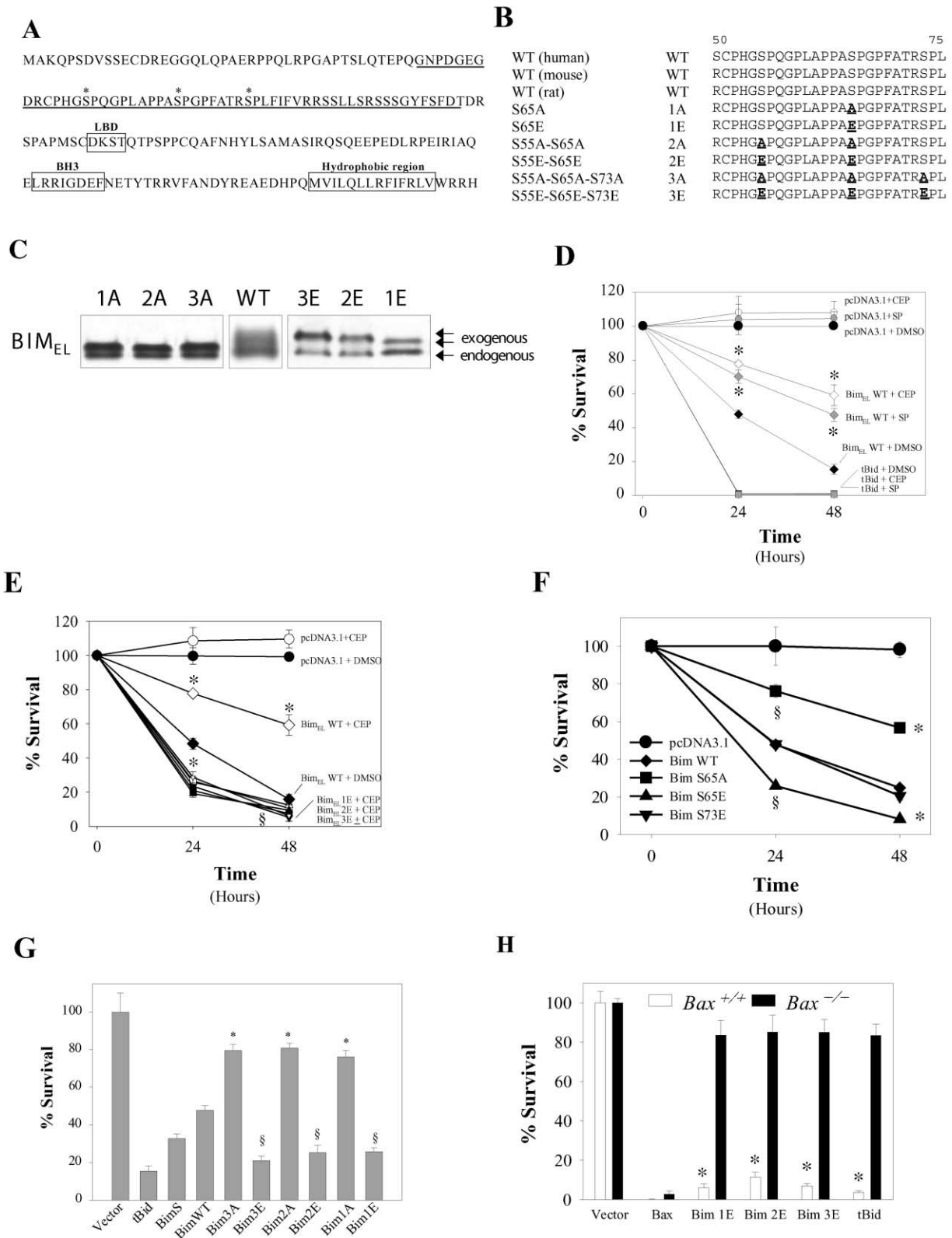
A

MAKQPSDVSSECDREGGQLQPAERPPQLRPGAPTSLQTEPQGNPDGEG

DRCPHGSPQGPLAPPASPGPFATRSPLFIFVRRSSLLSRSSSGYFSFDTDR

SPAPMSCDKSTQTPSPPCQAFNHYLSAMASIRQSQEEPEDLRPEIRIAQ

ELRRIGDEFNETYTRRVFANDYREAEDHPQMVILQLLRFIFRLVWRRH

B

		50 75
WT (human)	WT	SCPHGSPQGPLAPPASPGPFATRSPL
WT (mouse)	WT	RCPHGSPQGPLAPPASPGPFATRSPL
WT (rat)	WT	RCPHGSPQGPLAPPASPGPFATRSPL
S65A	1A	RCPHGSPQGPLAPPA**A**PGPFATRSPL
S65E	1E	RCPHGSPQGPLAPPA**E**PGPFATRSPL
S55A-S65A	2A	RCPHG**A**PQGPLAPPA**A**PGPFATRSPL
S55E-S65E	2E	RCPHG**E**PQGPLAPPA**E**PGPFATRSPL
S55A-S65A-S73A	3A	RCPHG**A**PQGPLAPPA**A**PGPFATRA**A**PL
S55E-S65E-S73E	3E	RCPHG**E**PQGPLAPPA**E**PGPFATRE**E**PL

C

D

E

F

G

H

Figure 2. Phosphorylation of BIM_EL Potentiates Its Proapoptotic Activity

(A) Amino acid sequence of murine BIM_EL showing the conserved LC8 binding domain (LBD), BH3 domain (BH3), and predicted hydrophobic region, as well as the region unique to BIM_EL (residues 42–97; underlined). Asterisks indicate the residues selected for site-directed mutagenesis.

(B) Schematic representation of the mutations introduced into BIM_EL.

vival in the CNS, in which BIM_{EL} phosphorylation occurs (Figures 1B and 1D). First, we cotransfected CGNs with *EGFP* and *Bim_{EL}* wt or *tBid* in the presence or absence of the MLK inhibitor CEP-1347 or the JNK inhibitor SP600125 and assessed cell survival (as indicated by the number of EGFP-positive cells). As shown in Figure 2D, both CEP-1347 and SP600125 attenuated cell death caused by overexpression of *Bim_{EL}* wt but not *tBid*, suggesting that the MLK/JNK-dependent phosphorylation of BIM_{EL} modulated its proapoptotic activity. Moreover, CEP-1347 did not inhibit cell death caused by overexpression of *Bim_{EL} 1E, 2E,* or *3E* (Figure 2E). Second, we cotransfected CGNs with *EGFP* and wt or mutant *Bim_{EL}* and assessed cell survival at multiple time points thereafter. As shown in Figures 2F and 2G, *Bim S65E* was more cytotoxic than *Bim* wt, which in turn was more cytotoxic than *Bim S65A*, at each time point examined. Of note, no statistically significant difference occurred among the *S65A* (*Bim 1A*), *S55A-S65A* (*Bim 2A*), and *S55A-S65A-S73A* (*Bim 3A*) mutants or among the *S65E* (*Bim 1E*), *S55E-S65E* (*Bim 2E*), and *S55E-S65E-S73E* (*Bim 3E*) mutants, at either 24 (Figure 2G) or 48 hr (data not shown). However, at each time point, the S→E mutants were more cytotoxic than *Bim* wt, which in turn was more cytotoxic than the S→A mutants (Figures 2F, 2G, and data not shown), indicating that BIM_{EL} phosphorylation enhances its proapoptotic activity. Finally, in separate experiments, neither the kinetics nor the extent of cell death induced by *Bim S73E* differed from that caused by *Bim* wt (Figure 2F). The observation that all of the Glu mutants were equally more cytotoxic than BIM_{EL} wt and that all of the Ala mutants were equally less cytotoxic than BIM_{EL} wt again suggests that Ser65 was a critical site for phosphorylation-dependent modulation of BIM_{EL}-mediated apoptosis.

Cell death caused by ectopic overexpression of *tBid, Bim,* or *Hrk* in CGNs requires BAX (Harris and Johnson, 2001; Putcha et al., 2002). To determine whether cell death induced by the most potent (i.e., the S→E) BIM_{EL} mutants remains BAX dependent, we cotransfected *$Bax^{-/-}$* CGNs with *EGFP* and *Bim 1E, Bim 2E, Bim 3E, tBid, Bax,* or *pcDNA3.1*. As shown in Figure 2H, only reintroduction of *Bax* killed *$Bax^{-/-}$* CGNs, indicating that cell death induced by overexpression of *Bim 1E, 2E,* or *3E* (or *tBid*) still requires BAX, consistent with our observation that BIM_{EL} phosphorylation occurs geneti-

cally upstream of (or in parallel with) the BAX/BCL-2 and caspase checkpoints.

Phosphorylation of BIM Does Not Alter Its Subcellular Localization or Integration into Mitochondrial Membranes

The sequestration of cell death effectors within distinct subcellular compartments has recently emerged as a common theme in the regulation of apoptosis. For example, in some nonneuronal cells, interaction with DLC1/LC8 sequesters BIM_{EL} to the microtubular dynein motor complex until certain apoptotic stimuli, such as UV irradiation or taxol, cause release of the BIM_{EL}-LC8 complex, allowing it to translocate to mitochondria and inactivate BCL-2 (Puthalakath et al., 1999). In SCG neurons, induced BIM_{EL} always localizes to mitochondria as an integral membrane protein (Putcha et al., 2001). We therefore hypothesized that the phosphorylation of BIM_{EL} may alter its proapoptotic activity by changing (1) its subcellular localization or (2) its integration into the outer mitochondrial membrane.

We tested this hypothesis using several approaches. First, we examined COS-7 cells expressing *YFP-Bim* wt, *YFP-Bim 3A,* and *YFP-Bim 3E*, using confocal microscopy. In each case, BIM colocalized with Mitotracker to mitochondria. We also observed no significant differences in this mitochondrial localization in either the presence or absence of 1.2 μM staurosporine (STS). (Figures 3A and 3B show representative images.) Next, we transiently transfected 293 cells with *Bim* wt, *Bim 3A,* or *Bim 3E* and examined the subcellular localization of BIM_{EL} by using subcellular fractionation. Moreover, to determine whether BIM_{EL} associated with mitochondria is integrated into mitochondrial membranes, we performed alkali extraction of the mitochondrial fractions. As shown in Figure 3C, neither the S→A nor the S→E mutations altered the mitochondrial localization of BIM or its integration into mitochondrial membranes. Finally, we obtained similar results for endogenous BIM_{EL} when we performed subcellular fractionation with alkali extraction in NGF-maintained, NGF-deprived/BAF-treated, and NGF-deprived/CEP-treated SCG neurons (Figure 3D). Taken together, these observations indicate that phosphorylation of BIM_{EL} did not alter its subcellular localization or integration into mitochondrial membranes.

(C) 293 cells were transiently transfected with *Bim_{EL}* wt or the indicated *Bim_{EL}* mutants. After 48 hr, extracts were prepared and examined by immunoblotting. For abbreviations for mutants (i.e., 1A, 2A, etc.), see panel (B).

(D) DIV5 rat CGNs were cotransfected with *EGFP* and the indicated vector. Immediately after transfection, cells were switched to K25 + S medium containing 0.1% DMSO, 1.3 μM CEP-1347, or 14 μM SP600125. The number of GFP-positive cells was counted at the indicated time points and expressed as a percentage of vector (pcDNA3.1)-transfected cells. Mean ± SD, n = 3–6 from two independent experiments (*p ≤ 0.001 versus wt + DMSO).

(E) DIV5 rat CGNs were cotransfected with *EGFP* and the indicated vector. Immediately after transfection, cells were switched to K25 + S medium containing 0.1% DMSO or 1.3 μM CEP-1347. The number of GFP-positive cells was counted at the indicated time points and expressed as a percentage of vector (pcDNA3.1)-transfected cells. Mean ± SD, n = 3–6 from two independent experiments (*p ≤ 0.001 versus wt + DMSO; §p ≤ 0.024).

(F) DIV5 rat CGNs were cotransfected with *EGFP* and the indicated vector. The number of GFP-positive cells was counted at the indicated time points and expressed as a percentage of vector (pcDNA3.1)-transfected cells. Mean ± SEM, n = 3 (*p ≤ 0.001 versus wt; §p = 0.002).

(G) DIV5 rat CGNs were cotransfected with *EGFP* and the indicated vector. The number of GFP-positive cells was counted at 24 hr and expressed as a percentage of vector (pcDNA3.1)-transfected cells. Mean ± SEM, n = 3 (*p ≤ 0.001 versus Bim_{EL} wt; §p ≤ 0.008).

(H) DIV5 CGNs from *$Bax^{+/+}$* or *$Bax^{-/-}$* mice were cotransfected with *EGFP* and the indicated vector. The number of GFP-positive cells was counted 48 hr later and expressed as a percentage of vector (pcDNA3.1)-transfected cells. Mean ± SD, n = 3–4 from two independent experiments (*p ≤ 0.001, *$Bax^{+/+}$* versus *$Bax^{-/-}$*).
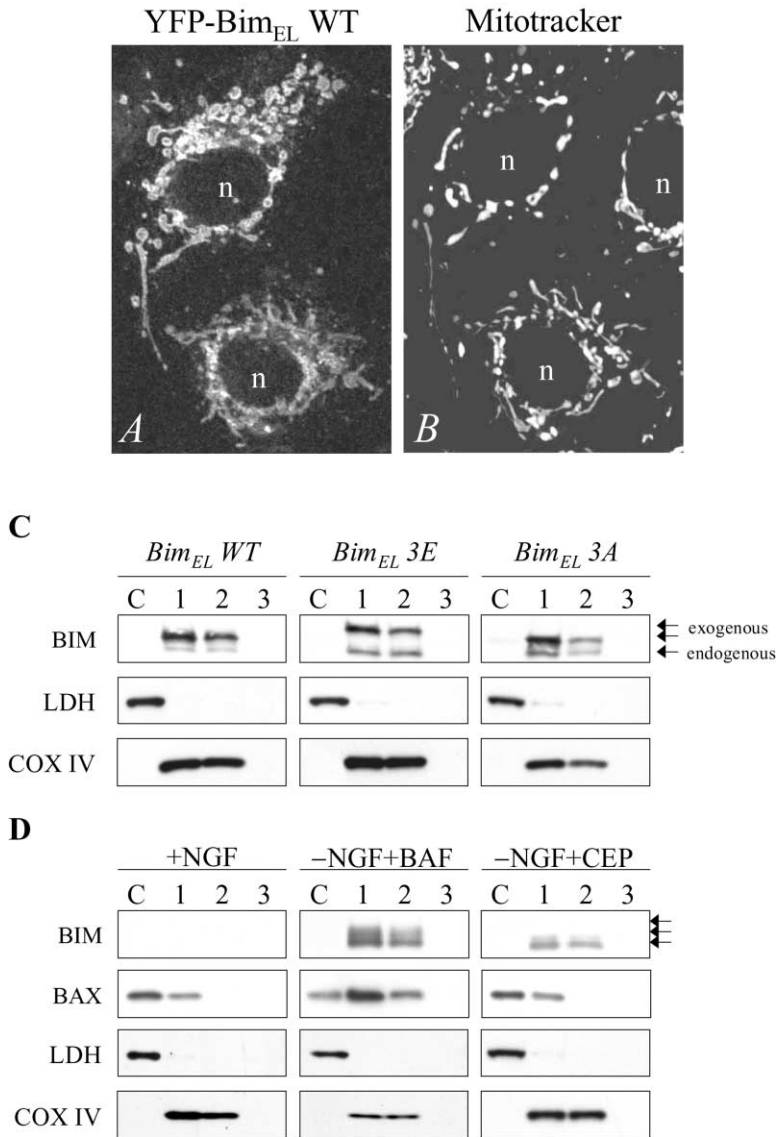
Figure 3. Phosphorylation of BIM_EL Does Not Alter Its Subcellular Localization or Integration into Mitochondrial Membranes

(A) COS-7 cells were transfected with *YFP-Bim_EL* wt, *YFP-Bim_EL 3A*, or *YFP-Bim_EL 3E* and visualized by using confocal microscopy. Since no differences were observed in the subcellular distribution of the different constructs in the presence or absence of 1.2 μM staurosporine, a representative image of untreated *YFP-Bim_EL* wt-transfected cells is shown. n, nucleus.

(B) Mitotracker staining in same field as (A).

(C) 293 cells were transfected with *Bim_EL* wt, *Bim_EL 3A*, or *Bim_EL 3E*. After 48 hr, the subcellular localization of BIM was examined by fractionation with alkali extraction by using 0.2 M Na_2CO_3 (pH 11.5). SDS (1% w/v) served as a positive control for the extraction of integral membrane proteins. Lactate dehydrogenase (LDH) and cytochrome oxidase subunit IV (COX IV) served as markers for the purity of cytosolic (C) and heavy membrane (HM) fractions, respectively, and as markers for equal protein loading. HM fractions were extracted with (1) isotonic buffer, (2) 0.2 M Na_2CO_3, or (3) 1% SDS. Resolution of the slower migrating bands of BIM_EL typically observed with transfection of *BimEL* wt were less pronounced in this particular experiment for a variety of technical reasons (e.g., gel composition).

(D) DIV5 SCG neurons were maintained in NGF, deprived of NGF in the presence of 50 μM BAF, or deprived of NGF in the presence of 400 nM CEP-1347 for 30 hr, and the subcellular localization of BIM was examined by fractionation with alkali extraction as in (C). Of note, consistent with its inhibition of BIM and HRK induction, CEP-1347 prevented BAX translocation and integration into mitochondrial membranes as predicted by the dynamic equilibrium model of protein translocation (Putcha et al., 2002).

Mitochondrially Localized JNKs but Not Their Upstream Activators MLKs or MKKs Phosphorylate BIM

Because the MLK/JNK pathway inhibitors CEP-1347 and SP600125 prevented phosphorylation of BIM_EL (Figures 1E, 1F, 3D, and data not shown), we began our search for the putative BIM_EL kinase among the kinases of this pathway. We performed an in vitro kinase assay with GST-BIM_EL wt and GST-BIM_EL 3A to test the following candidate kinases directly: MLK1–3, MKK4, MKK7, and JNK1–3. All kinases tested were able to phosphorylate themselves (Figure 4A), indicating activity in the kinase reactions, and the identity of the GST-BIM_EL band was confirmed by immunoblotting (data not shown). MKK7 did not phosphorylate BIM_EL wt, whereas MLK1-3 and MKK4 phosphorylated BIM_EL wt, but showed no selectivity for Ser55, 65, and/or 73 (i.e., wt and 3A equally phosphorylated). In contrast, JNK1, JNK3, and to a lesser extent, JNK2 demonstrated significant selectivity for these sites, with a 70%–85% decrease in the amount

of ^{32}P incorporated into BIM_EL 3A versus BIM_EL wt (Figures 4B and 4C). Moreover, the electrophoretic mobility of BIM_EL decreased when JNKs were incubated with BIM_EL wt as compared with BIM_EL 3A (Figure 4A and data not shown), consistent with phosphorylation. Thus, JNK1-3 but not MLK1-3, MKK4, or MKK7 phosphorylated BIM_EL selectively at Ser55, 65, and/or 73 in vitro, consistent with our previous observation that either the MLK inhibitor CEP-1347 or the JNK inhibitor SP600125 prevented BIM_EL phosphorylation (Figures 1E and 1F).

Since the cell death assays in CGNs (Figures 2F and 2G) strongly suggested that Ser65 was a critical site for phosphorylation-dependent modulation of BIM-mediated proapoptotic activity, we examined whether JNK-mediated phosphorylation of BIM_EL exhibited similar site specificity in the in vitro kinase assay. As shown in Figure 4C, ^{32}P incorporation was decreased significantly (~70%–80%) in the Ala mutants as compared with BIM_EL wt, consistent with our previous results (Figures 4A and 4B) demonstrating that JNKs specifically phosphorylate

BIM_{EL} at Ser55, 65, and/or 73. Moreover, the extent of reduction of ^{32}P incorporation was equivalent among the 1A (S65), 2A (S55/S65), and 3A (S55/S65/S73) mutants, indicating that Ser65 was the site specifically phosphorylated by JNKs, consistent with the functional studies in CGNs (Figures 2F and 2G). In sum, the results from Figures 1–4 demonstrate that JNKs specifically phosphorylated BIM_{EL} at Ser65, enhancing its proapoptotic activity.

Finally, since BIM_{EL} localizes primarily, if not exclusively, to mitochondria in NGF-deprived SCG neurons, we examined the subcellular distribution of components of the MLK/JNK signaling pathway by subcellular fractionation in NGF-maintained, NGF-deprived/BAF-treated, and NGF-deprived/CEP-treated SCG neurons. As shown in Figure 4D, MLK3, MKK7, and JIP3 were found in the heavy membrane fraction enriched in mitochondria, while total and phospho-JNK were cytosolic, nuclear, and mitochondrial (Figure 4D and data not shown). Although MKK4 also localized to mitochondria and translocated to the nucleus with NGF withdrawal, phospho-MKK4 appeared only in the nucleus with TFD, suggesting that MKK7, not MKK4, mediates activation of mitochondrial JNKs, leading to BIM_{EL} phosphorylation. Moreover, the observation that CEP-1347 inhibits phosphorylation and nuclear translocation of MKK4 suggests that phosphorylation modulates its subcellular localization as with other MAPKs (Khokhlatchev et al., 1998). In sum, these data indicate that components of the MLK/JNK signaling cascade are appropriately localized to mediate BIM phosphorylation.

Of interest, we found some c-Jun and P-cJun associated with the mitochondrial fraction of NGF-deprived SCG neurons, consistent with other recent reports of mitochondrial localization of active AP-1 complexes (Haase et al., 1997; Ogita et al., 2002). Although the majority of P-cJun clearly resides in the nucleus, it is intriguing to speculate whether this observation reflects a genuine extranuclear role for c-Jun either in mitochondrial gene expression (Ogita et al., 2002) or in proapoptotic signaling at mitochondria (Li et al., 2000).

Finally, to examine further the site specificity of BIM_{EL} phosphorylation, we generated a phospho-specific antibody that recognizes phospho-Ser65 BIM_{EL} (P-BIM). This antibody detected recombinant BIM_{EL} phosphorylated in vitro by JNKs (Figure 4E) at Ser65 (Figure 4F), as well as endogenous BIM_{EL} phosphorylated during TFD in SCG neurons in a CEP-inhibitable manner (Figure 4G).

Inhibition of MLK/JNK Signaling Attenuates TFD-Induced Apoptosis

CEP-1347-mediated inhibition of the MLK/JNK pathway prevents NGF deprivation-induced apoptosis long-term in SCG neurons (Maroney et al., 1999; Harris et al., 2002a) and significantly attenuates TFD-induced CGN death (Trotter et al., 2002; Harris et al., 2002b). To evaluate further the contributions of MLKs and JNKs to trophic factor withdrawal-induced cell death in rat CGNs, we transiently cotransfected K25 + S-maintained CGNs with EGFP and previously characterized (Xu et al., 2001) kinase-inactive versions of Mlk2 (K125A), Mlk3 (K144R), Mkk4 (K113A), and Jnk1 (K55A). After 48 hr, the cells

were then maintained in K25 + S or switched to K5 − S, and the number of GFP-positive cells were counted by a naïve observer. As shown in Figure 5, the kinase-inactive forms of Mlk2, Mlk3, and to a lesser extent, Jnk1 inhibited TFD-induced CGN death, consistent with recent reports in SCG and CG neurons and neuronal PC12 cells (Mota et al., 2001; Xu et al., 2001; Trotter et al., 2002). Thus, inhibition of the MLK/JNK pathway by both molecular genetic and pharmacological approaches significantly attenuates CGN apoptosis after trophic factor withdrawal.

Neuronal Cell Death Induced by Activation of the MLK/JNK Pathway Requires BIM and BAX but Not BID

Many cell death stimuli, including TFD, activate the MLK/JNK pathway; overexpression of kinases of this signaling module induces cyt c release, caspase activation, and cell death in neuronal PC12 cells and SCG neurons (Mota et al., 2001; Xu et al., 2001). Moreover, since kinase-inactive mutants of MLKs, MKK4, and JNK1 attenuated TFD-induced apoptosis in CGNs (Figure 5 and data not shown), we sought to characterize cell death induced by transient transfection of wild-type Mlk2, Mlk3, Mkk4, Mkk7, or Jnk1 in K25 + S-maintained rat CGNs. As shown in Figures 6 and 7, overexpression of any of these kinases caused cell death in CGNs, even in the presence of K25 + S, overriding any endogenous antiapoptotic signals.

Our finding that overexpression of wild-type Jnk1-, Mkk4-, or Mkk7-induced cell death in CGNs may appear to conflict with a recent report showing that wild-type Jnk1 does not kill CHO cells (Lei et al., 2002); however, several technical points may explain these observations. First, unlike most, if not all, nonneuronal cells, CGNs (and CNS neurons more generally) possess very high constitutive JNK and MKK activity (Xu et al., 1997; Eilers et al., 1998; Coffey et al., 2000, 2002). Second, in these neurons, transfection itself causes some activation of the MLK/JNK pathway, consistent with the cytoprotective effects of CEP-1347, SP600125, and kinase-inactive mutants of Mlk2, Mlk3, Mkk4, and Jnk1 in pcDNA3.1-transfected CGNs (Figures 2D, 2E, 5, and data not shown). Finally, transfection of these neurons requires incubation of the cells in serum-free medium for 1.5–3 hr, which in itself causes activation of the MLK/JNK pathway (Miller et al., 1997a; Eilers et al., 1998; Coffey et al., 2002). In sum, these findings explain why overexpression of wild-type Jnk1, Mkk4, or Mkk7 induces cell death in CGNs. Moreover, taken together with the aforementioned reports, our observations suggest that this susceptibility may characterize CNS neurons more generally, revealing a potentially clinically important difference between these neurons and other cells.

We also evaluated further the specificity of the MLK/JNK pathway inhibitor CEP-1347. CEP-1347 selectively inhibits MLKs but not several other kinases (e.g., MEKK1, TPL-2, ASK1, MKK4, and MKK7) in various in vitro assays (Maroney et al., 2001; Xu et al., 2001). Based on these findings, we hypothesized that CEP-1347 should inhibit CGN cell death caused by MLKs but not by downstream kinases, such as MKK4, MKK7, and JNK1. Therefore, we cotransfected 5 days in vitro (DIV),
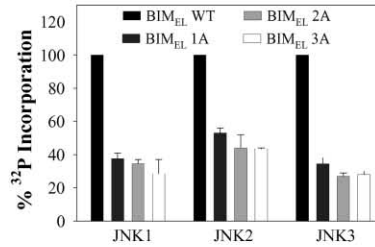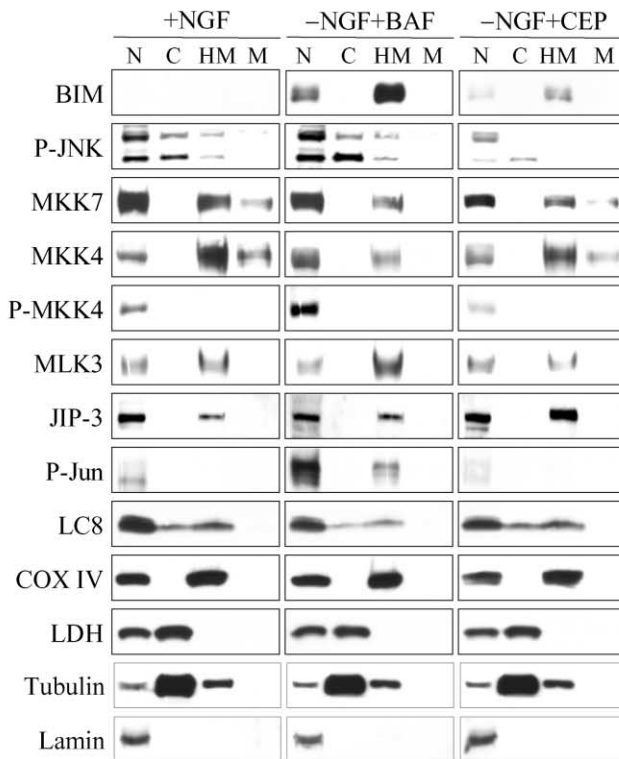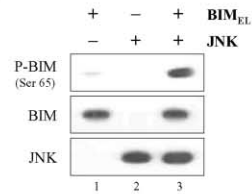
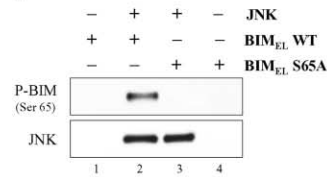**A**
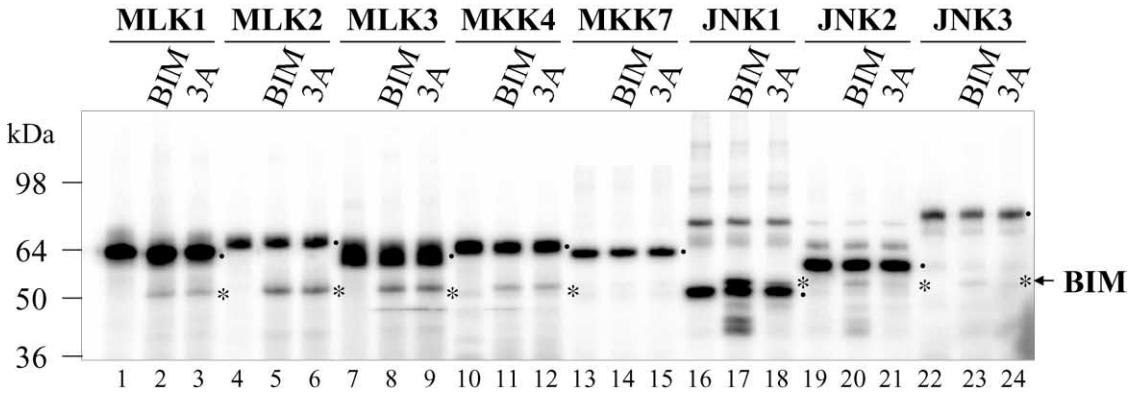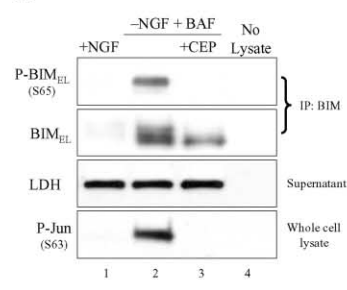

B
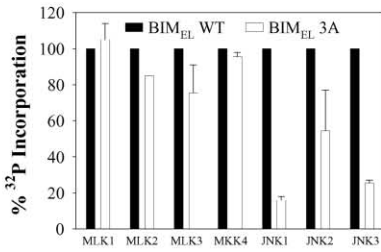
C

D

E

F

G

Figure 4. Mitochondrially Localized JNKs but Not Their Upstream Activators MLKs or MKKs Phosphorylate BIM$_{EL}$ at Ser65

(A) BIM$_{EL}$ wt (BIM) or S55A/S65A/S73A (3A) was incubated with MLK1 (lanes 1–3), MLK2 (lanes 4–6), MLK3 (lanes 7–9), MKK4 (lanes 10–12), MKK7 (lanes 13–15), JNK1 (lanes 16–18), JNK2 (lanes 19–21), or JNK3 (lanes 22–24) together with [γ-^{32}P]ATP for an in vitro kinase assay. The
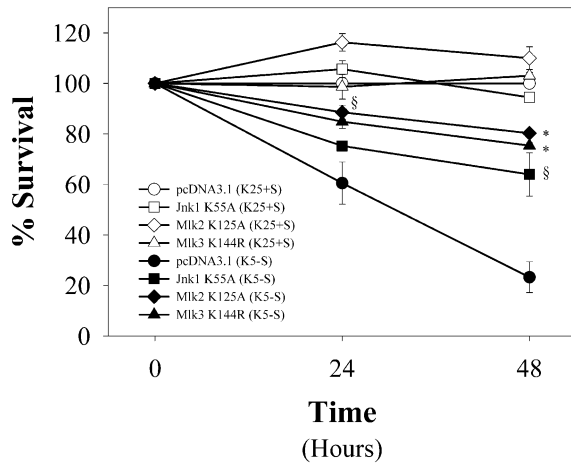
Figure 5. Inhibition of MLK/JNK Signaling Attenuates TFD-Induced Apoptosis

DIV5 rat CGNs were cotransfected with EGFP and the indicated vector. After 48 hr, cells were maintained in K25 + S or switched to K5 − S. Then, the number of GFP-positive cells was counted by a naïve observer at the indicated time points and expressed as a percentage of vector (pcDNA3.1)-transfected cells. Mean ± SEM, n ≥ 3 (*p ≤ 0.001 versus pcDNA3.1, K5 − S; §p ≤ 0.024).

K25 + S-maintained rat CGNs with *EGFP* and *Mlk2*, *Mlk3*, *Mkk4*, *Mkk7*, or *Jnk1* and then added CEP-1347 to the medium. As shown in Figure 6B, CEP-1347 significantly inhibited cell death caused by *Mlk2* and *Mlk3* but not that induced by *Mkk4*, *Mkk7*, or *Jnk1*.

The mitochondrial substrates for MLK/JNK signaling remain unknown. Recently, Tournier et al. (2000) proposed that another BH3-only protein, BID (or tBID), may mediate proapoptotic signaling by JNKs. Therefore, we transiently cotransfected DIV5 CGNs from *Bid*^{+/+} or *Bid*^{−/−} mice with *EGFP* and *Mlk3* and assessed cell survival over the ensuing 48 hr. As shown in Figure 7A, *Bid* deletion did not change the kinetics or extent of cell death caused by overexpression of *Mlk3*. Similar findings were obtained with other kinases of the MLK/JNK

pathway, including *Mlk2*, *Mkk4*, and *Jnk1* (data not shown).

Taken together with previous studies (Harris and Johnson, 2001; Putcha et al., 2001; Whitfield et al., 2001), our current findings implicate BH3-only proteins, such as BIM and HRK, as two likely targets, which function genetically upstream of the BAX/BCL-2 checkpoint to induce mitochondrial apoptogen release, caspase activation, and apoptosis. Therefore, we hypothesized that maximal cell death caused by activation of the MLK/JNK pathway requires BIM. To test this hypothesis, we transiently cotransfected DIV5 CGNs from *Bim*^{+/+}, *Bim*^{+/−}, or *Bim*^{−/−} mice with *EGFP* and *Mlk2*, *Mlk3*, *Mkk4*, or *Jnk1* and assessed cell survival over the next 48 hr. As shown in Figures 7B–7E, *Bim* deletion, in contrast to *Bid* deficiency (Figure 7A), attenuated cell death caused by overexpression of kinases of the MLK/JNK pathway in a gene dose-dependent manner.

Finally, activation of the MLK/JNK pathway induced phosphorylation of BIM_{EL} (Figure 1) and cell death in K25 + S-maintained CGNs (Figures 6 and 7A–7E), and cell death caused by overexpression of S→E mutants designed to mimic constitutive phosphorylation of BIM_{EL} required BAX (Figure 2F). Therefore, we postulated that cell death caused by activation of the MLK/JNK pathway requires BAX. To test this hypothesis, we transiently cotransfected DIV5 CGNs from *Bax*^{+/+} or *Bax*^{−/−} mice with *EGFP* and *Mlk2*, *Mlk3*, *Mkk4*, *Mkk7*, or *Jnk1* and assessed cell survival 48 hr later. As shown in Figure 7F, *Bax* deletion prevented cell death caused by overexpression of kinases of the MLK/JNK pathway.

Discussion

JNKs Regulate BIM Transcriptionally and Posttranslationally

Based on the current literature and evidence presented in this paper, two potentially interrelated mechanisms regulate BIM_{EL} function posttranslationally: sequestration to microtubules by interaction with LC8 (Puthalakath et al., 1999) and JNK-dependent phosphorylation.

position of GST-BIM_{EL} is indicated on the right (and by asterisks), and the autophosphorylated kinases are indicated by a filled dot to the right.

(B) Quantification of the ^{32}P incorporation into BIM_{EL} proteins in the kinase assay shown in (A). The percentage of ^{32}P incorporation into BIM_{EL} 3A is expressed relative to that into BIM_{EL} wt, which was set to 100%. Data are the mean ± SEM from duplicate samples from two independent experiments.

(C) BIM_{EL} wt (BIM), S65A (1A), S55A/S65A (2A), or S55A/S65A/S73A (3A) was incubated with JNK1, JNK2, or JNK3 together with [γ-^{32}P]ATP for an in vitro kinase assay, and the ^{32}P incorporation into BIM_{EL} proteins was quantified. The percentage of ^{32}P incorporation into BIM_{EL} 1A, 2A, or 3A is expressed relative to that into BIM_{EL} wt, which was set to 100%. Data are the mean ± SEM from duplicate samples from two independent experiments.

(D) DIV5 SCG neurons were maintained in NGF, deprived of NGF in the presence of 50 μM BAF, or deprived of NGF in the presence of 400 nM CEP-1347 for 30 hr, and the subcellular localization of the indicated proteins was examined by fractionation. (C, cytosol; HM, heavy membrane; M, microsomes; N, nucleus) Please note that most, if not all, nonnuclear proteins are also present in the "nuclear" fraction because in this (and most) fractionation protocols, the nuclear fraction contains some intact cells unless further resolved.

(E) Western blot analysis of anti-phospho-BIM_{EL} (Ser65) antibody. Recombinant BIM_{EL} wt was incubated with JNK1 and analyzed by immunoblotting (10 μg loaded per lane) with the indicated antibodies. Note that the anti-phospho-BIM (Ser65) antibody did not recognize unphosphorylated BIM_{EL} (lane 1) or autophosphorylated JNK (lane 2).

(F) Anti-phospho-BIM_{EL} (Ser65) antibody recognizes BIM_{EL} phosphorylated at Ser65. Recombinant BIM_{EL} wt or S65A was incubated with JNK1 and analyzed by immunoblotting (10 μg loaded per lane) with the anti-phospho-BIM_{EL} (Ser65) antibody. Note that the antibody recognized phosphorylated BIM_{EL} wt (lane 2) but not the S65A mutant (lane 3).

(G) DIV5 SCG neurons were maintained in NGF, deprived of NGF in the presence of 50 μM BAF, or deprived of NGF in the presence of 400 nM CEP-1347. After 24 hr, BIM was immunoprecipitated; in parallel, whole-cell extracts were prepared. Then immunoprecipitates, supernatants, and whole-cell lysates were analyzed by Western blotting with the indicated antibodies.
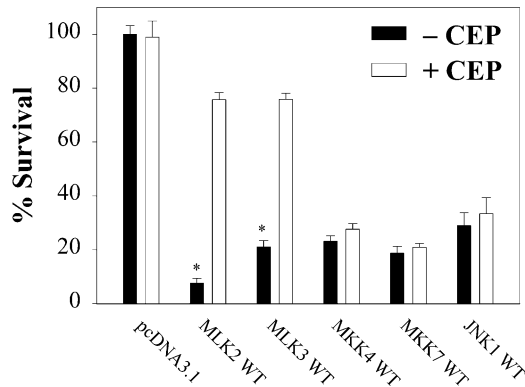
A
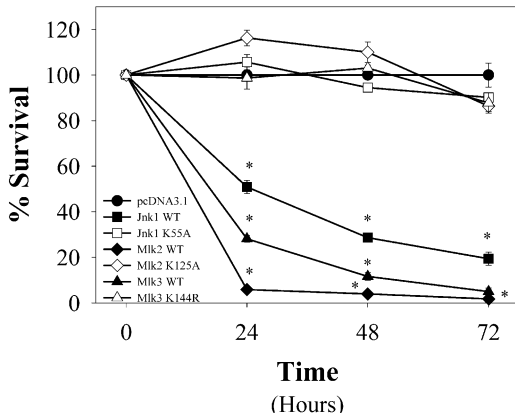
B

Figure 6. Activation of MLK/JNK Signaling Causes Neuronal Cell Death

(A) DIV5 rat CGNs were cotransfected with EGFP and the indicated vector. The number of GFP-positive cells was counted by a naïve observer at the indicated time points and expressed as a percentage of vector (pcDNA3.1)-transfected cells. Mean ± SEM, n ≥ 3 (*p ≤ 0.001 versus pcDNA3.1).

(B) DIV5 rat CGNs were cotransfected with EGFP and the indicated vector. After transfection, the cells were maintained in K25 + S or switched to K25 + S medium containing 1.3 μM CEP-1347. Then, the number of GFP-positive cells was counted by a naïve observer 48 hr later and expressed as a percentage of vector (pcDNA3.1)-transfected cells. Mean ± SEM, n = 3 (*p ≤ 0.001, −CEP versus +CEP).

At least in neurons, the role of LC8 in regulating BIM_{EL} function is unknown. First, by subcellular fractionation, LC8 is distributed in multiple subcellular compartments in both NGF-maintained and -deprived SCG neurons (Figure 4D), consistent with previous reports (Puthalakath et al., 1999). In contrast, when induced in these neurons, BIM_{EL} is found only at mitochondria (Putcha et al., 2001; Figure 4D). Second, whether endogenous BIM_{EL} and LC8 interact in primary neurons and whether this interaction changes with TFD remains unclear. Finally, although Ser65 lies outside the LC8 binding domain (residues 107–110; Figure 2A), whether these re-

gions are juxtaposed in the tertiary structure is unknown. However, one intriguing observation suggests that JNK-mediated BIM_{EL} phosphorylation and sequestration by LC8 may not be mutually exclusive regulatory mechanisms: JNK1/2, BIM, and LC8 colocalize to the heavy membrane fractions enriched for mitochondria (Figure 4D and data not shown).

Several lines of evidence indicate that JNKs phosphorylate BIM_{EL} at Ser65. First, activation of the MLK/JNK pathway occurs with kinetics consistent with the time course of BIM_{EL} phosphorylation in SCG (Figure 1A) (Mota et al., 2001) and CG neurons (Figure 1B). Second, the MLK inhibitor CEP-1347 (Figures 1E and 3D) and the JNK inhibitor SP600125 (Figure 1F) prevented BIM_{EL} phosphorylation. Third, recombinant JNK1–3 but not MLK1–3, MKK4, or MKK7 phosphorylated recombinant BIM_{EL} selectively at Ser65 (Figures 4A–4C). Fourth, an anti-phospho-Ser65 antibody reacted specifically with BIM_{EL} phosphorylated at Ser65 in vitro by JNK1 (Figures 4E and 4F) and during TFD in SCG neurons in a CEP-inhibitable manner (Figure 4G). Finally, at least in the paradigms examined, JNKs and their upstream activators were appropriately localized to mediate BIM_{EL} phosphorylation (Figure 4D).

Moreover, several observations demonstrate that the phosphorylation of BIM_{EL} is a physiologically important mechanism for enhancing its proapoptotic activity. First, BIM_{EL} became phosphorylated during TFD in SCG and CG neurons (Figure 1). Second, abrogation of this phosphorylation with the MLK inhibitor CEP-1347 prevented TFD-induced apoptosis in the former (Maroney et al., 1999; Harris et al., 2002a) and significantly attenuated K5 − S-induced cell death in the latter (Trotter et al., 2002; Harris et al., 2002b). Third, the MLK inhibitor CEP-1347 and the JNK inhibitor SP600125 both attenuated cell death induced by overexpression of Bim_{EL} wt in CGNs (Figures 2D and 2E). Fourth, Bim_{EL} S65E and S65A, which mimic constitutive phosphorylation and dephosphorylation, respectively, induced CGN death more and less efficiently, respectively, than Bim_{EL} wt (Figures 2F and 2G). Since this death occurred in the presence of K25 + S, these observations suggest that overexpression of Bim_{EL} in this setting overcame endogenous anti-apoptotic signals, such as those provided by PI3K/Akt and Ras/MEK. Nonetheless, cell death induced by Bim_{EL} S65E, S55E/S65E, or S55E/S65E/S73E still required the multidomain proapoptotic BCL-2 protein BAX (Figure 2H), consistent with our earlier findings that BIM functions genetically upstream of the BAX/BCL-2 and caspase checkpoints (Putcha et al., 2001) and suggesting that overexpression of Bim_{EL} in this setting engaged physiological apoptotic pathways. Further delineation of the relative contributions of transcriptional and post-translational mechanisms to the regulation of BIM's pro-apoptotic activity will require generation of mutant animals (e.g., S65A "knockin" mice).

The mechanism(s) by which phosphorylation affects the proapoptotic activity of BIM_{EL} is unclear. Numerous possibilities exist, including changes in BIM's subcellular localization, mitochondrial membrane integration, stability, or interactions with other known or unknown proteins. Because phosphorylation of BIM_{EL} did not alter its subcellular localization or integration into mitochondrial membranes (Figures 3A–3D), we are currently in-

vestigating other possible mechanisms, including those mentioned above (i.e., stability and protein-protein interactions).

Our findings highlight once again the critical role of subcellular localization in regulating signal transduction in general and the MLK/JNK pathway in particular, consistent with recent reports suggesting that JNK1 and JNK2/3 coexpressed in CGNs are (1) differentially activated by TFD (with JNK1 possessing high constitutive/low inducible activity and JNK2/3 possessing low constitutive/high inducible activity), (2) differentially localized (JNK1 being extranuclear and JNK2/3 being nuclear), and (3) differentially responsible for nuclear c-Jun phosphorylation (Coffey et al., 2000, 2002). Although we did not see evidence for the dynamic regulation of the subcellular localization of JNK1/2, MLK3, MKK7, or JIP3 with TFD in SCG neurons, we caution that our findings should not be taken to indicate that such regulation does not exist, because of limitations inherent to these experiments (e.g., isoform specificity of antibodies). Based on our observations and recent reports (Coffey et al., 2000, 2002), we propose (Figure 8) that TFD in SCG and CG neurons causes activation of MLKs and MKK4/7, leading to activation of nuclear JNKs (presumably JNK2/3), which likely mediate the transcription-dependent (e.g., AP-1-mediated) proapoptotic effects of JNKs in this paradigm (e.g., BIM and HRK induction). In parallel, MLK/MKK-dependent activation of extranuclear JNKs (primarily JNK1) culminates in transcription-independent effects, including phosphorylation of cellular substrates, such as BIM.

In addition to posttranslational regulation, an important mechanism for regulating BIM function during TFD in neuronal and hematopoietic cells appears to be transcriptional (Dijkers et al., 2000; Harris and Johnson, 2001; Putcha et al., 2001; Whitfield et al., 2001; Dijkers et al., 2002). However, the specific signaling pathways responsible for this transcriptional control vary in a cell type- and stimulus-specific manner. For example, NGF-deprived SCG neurons rely primarily on *activation* of the MLK/JNK pathway culminating in AP-1-dependent transactivation of BIM (Figures 1E, 3D, and 4D) (Harris and Johnson, 2001; Putcha et al., 2001; Whitfield et al., 2001), with some modest contribution from loss of PI3K/Akt and Ras/MEK signaling (Putcha et al., 2001; see below). In contrast, in IL-3-deprived hematopoietic cells, *suppression* of the PI3K/Akt pathway culminating in FKHRL1-mediated BIM transcription predominates (Dijkers et al., 2000, 2002), with some contribution again from loss of Ras/MEK signaling (Shinjyo et al., 2001).

However, conclusions based on these reports that activation of MLK/JNK signaling and/or suppression of PI3K/Akt and Ras/MEK signaling are the only pathways controlling BIM transcription likely underrepresent the complexity of BIM transcriptional control. First, Liu and Greene (2001) reported that Rb-dependent, E2F-mediated gene repression attenuates TFD-induced apoptosis in SCG neurons and that depression of certain E2F target genes, such as B- and C-myb, which are induced by NGF deprivation in these neurons (Estus et al., 1994), can induce cell death in these neurons. Since the BIM promoter contains potential binding sites for c-Myb (Bouillet et al., 2001), BIM may be one of the E2F target genes derepressed during TFD. Second, even within a

single cell type, control of BIM transcription may vary according to cellular context. For example, in the case of mass cultures of NGF-maintained SCG neurons, inhibition of the Ras/MEK or PI3K/Akt pathway by using U0126 or LY294002, respectively, causes modest MLK/JNK-*dependent* induction of BIM (Putcha et al., 2001); however, in the context of depolarization-induced survival of both SCG and CG neurons, which depends almost exclusively on PI3K/Akt signaling (Crowder and Freeman, 1999; Vaillant et al., 1999; Dudek et al., 1997; Miller et al., 1997b), LY294002 alone causes significant MLK/JNK-*independent* BIM induction (G.V.P. and E.M.J., unpublished data) and BAX-dependent cell death (Miller et al., 1997a), consistent with physiological crosstalk between the Ras/MEK, PI3K/Akt, and MLK/JNK pathways. Thus, coordinate transcriptional regulation of BH3-only proteins, such as that seen with BIM and HRK during neuronal apoptosis, will likely involve complex signaling networks.

### Intrinsic Pathway Apoptotic Signaling Mediated by MLKs, MKKs, and JNKs Requires BIM and BAX but Not BID

Many apoptotic stimuli, such as TFD and UV irradiation, activate JNKs, which in turn trigger apoptosis via the intrinsic pathway by transcription-dependent and/or transcription-independent mechanisms. Taken together with recent reports (Lindsten et al., 2000; Harris and Johnson, 2001; Wei et al., 2001; Zong et al., 2001; Lei et al., 2002; Putcha et al., 2002), our findings (Figure 7F) indicate that both pathways eventually require BAX, BAK, and/or BOK-dependent release of mitochondrial apoptogens for caspase activation and cell death, though coexpression of these multidomain proapoptotic BCL-2 proteins does not guarantee functional redundancy (LeBlanc et al., 2002; Putcha et al., 2002).

However, targets for JNK signaling upstream of the BAX/BCL-2 (or mitochondrial) checkpoint are unknown. One potential target is BH3-only proteins, which appear to function as "sensors," transducing death signals and activating mitochondrial effectors, such as BAX, at least in part by relieving inhibition by multidomain antiapoptotic BCL-2 proteins (e.g., BCL-2 and BCL-X$_L$). Accordingly, BID (or tBID) was previously proposed as a possible mitochondrial target of JNK-mediated apoptosis during UV-induced (transcription-independent) cell death in MEFs (Tournier et al., 2000). However, taken together with other recent reports (Harris and Johnson, 2001; Putcha et al., 2001; Whitfield et al., 2001; Lei et al., 2002), data presented in this paper strongly suggest that BIM (and perhaps HRK), not BID or tBID, is a likely target of transcription-dependent and/or transcription-independent JNK-mediated apoptotic signaling (Figure 8). First, inhibition of MLK/JNK signaling by either molecular genetic or pharmacologic means attenuates BIM expression (Harris and Johnson, 2001; Putcha et al., 2001; Whitfield et al., 2001), phosphorylation (Figures 1E, 3D, and 4D), and proapoptotic activity (Figures 2D and 2E), and prevents TFD-induced apoptosis (Figure 5) (Estus et al., 1994; Ham et al., 1995; Maroney et al., 1999; Xu et al., 2001). Second, the converse is true for activation of MLK/JNK signaling (Figures 6, 7, and data not shown). Finally, *Bim* (but not *Bid* or *Bad*) deletion
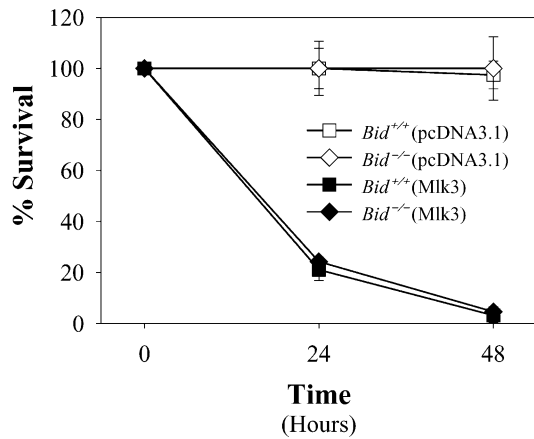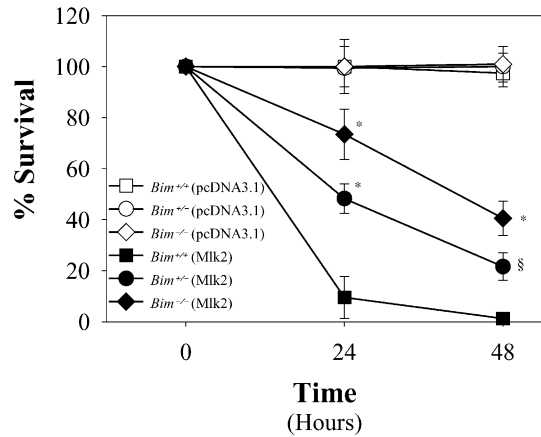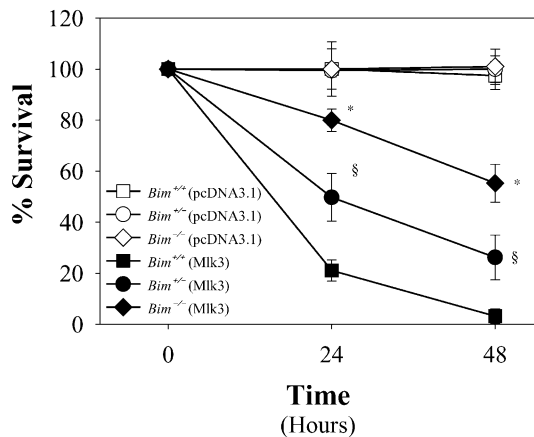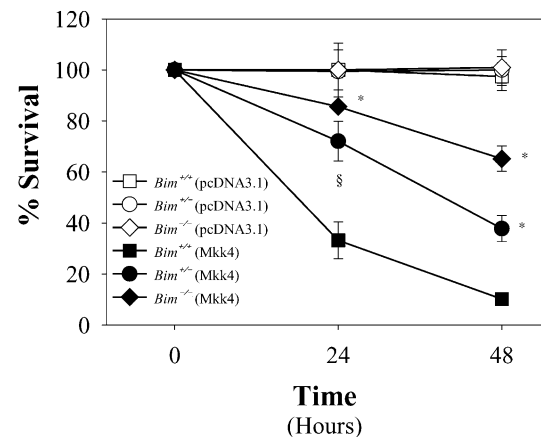
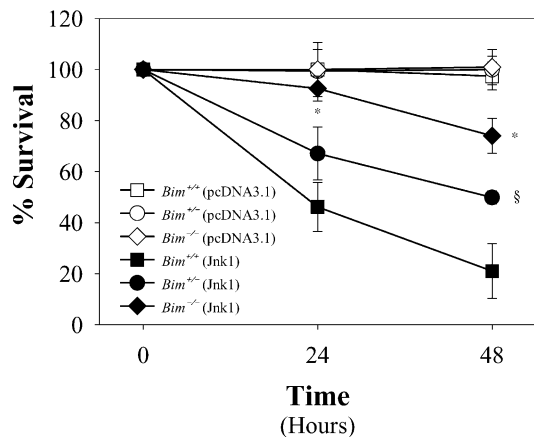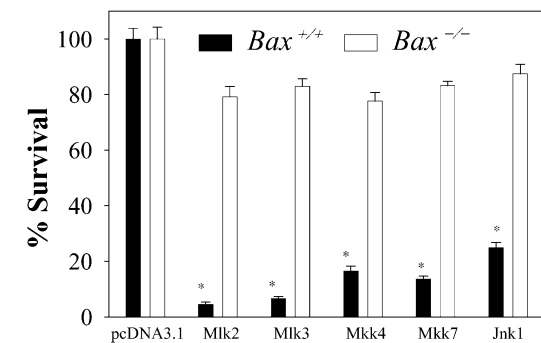Figure 7. Neuronal Cell Death Induced by Activation of the MLK/JNK Pathway Requires BIM and BAX but Not BID

(A) DIV5 CGNs from $Bid^{+/+}$ or $Bid^{-/-}$ mice were cotransfected with $EGFP$ and $Mlk3$. The number of GFP-positive cells was counted at the indicated times and expressed as a percentage of vector (pcDNA3.1)-transfected cells. Mean ± SD, n = 3–4 from two independent experiments.
(B–E) DIV5 CGNs from $Bim^{+/+}$, $Bim^{+/-}$, or $Bim^{-/-}$ mice were cotransfected with EGFP and the indicated vector. The number of GFP-positive cells was counted over the ensuing 48 hr and expressed as a percentage of vector (pcDNA3.1)-transfected cells. Mean ± SD, n = 3–4 from two independent experiments (*p ≤ 0.001 versus $Bim^{+/+}$. §p = 0.002 in B, p ≤ 0.008 in C, p = 0.030 in D, and p = 0.007 in E).
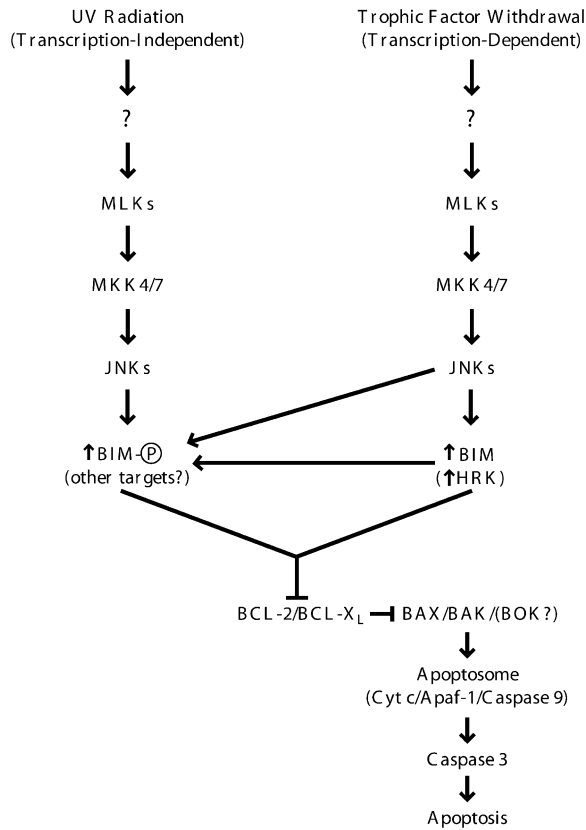
Figure 8. Model: Proposed Genetic and Biochemical Pathway for Transcription-Dependent and -Independent JNK-Induced Apoptosis

In brief, TFD in SCG and CG neurons causes activation of MLKs and MKK4/7, leading to activation of nuclear JNKs (probably JNK2/3), which likely mediate the transcription-dependent (e.g., AP-1-mediated) proapoptotic effects of JNKs in this paradigm (e.g., BIM and HRK induction). In parallel, MLK/MKK-dependent activation of extranuclear JNKs (primarily JNK1) culminates in transcription-independent effects, including phosphorylation of cellular substrates, such as BIM. The upstream activators of MLKs are presently unclear, but may include small GTPases (e.g., cdc42/rac1) and/or germinal center kinase (GCK) family kinases. Further delineation of the relative contributions of transcriptional and posttranslational mechanisms to the regulation of BIM's proapoptotic activity will require generation of mutant animals (e.g., S65A knockin mice).

attenuates but does not prevent cell death caused by TFD (Putcha et al., 2001, 2002) or by activation of MLK/ JNK signaling in a gene dose-dependent manner (Figure 7), consistent with functional redundancy among BH3-only proteins, likely BIM and HRK in neurons, genetically downstream of JNKs (and upstream of BAX) during apoptosis. Thus, consistent with the emerging role for BH3-only proteins as sensors that transduce death signals to mitochondrial effectors, BIM—and presumably HRK—represents important new mitochondrial targets for transcription-dependent and/or -independent JNK-medi-

ated proapoptotic signaling, leading to BAX-dependent apoptogen release, caspase activation, and cell death.

Experimental Procedures

Reagents

All reagents were purchased from Sigma unless otherwise stated. Other reagents and their sources were collagenase and trypsin (Worthington Biochemical); caspase inhibitor boc-aspartyl(OMe)-fluoromethylketone (BAF) (Enzyme Systems Products); and recombinant active MKK4, MKK7, JNK1, and JNK2α2 (Upstate Biotechnology, Inc.). Recombinant mixed lineage kinases (MLKs) and JNK3α1 were made as described elsewhere (Le et al., 2001). Medium lacking NGF (AM0) consisted of Eagle's MEM with Earle's salts (Invitrogen) supplemented with 10% fetal bovine serum, 2 mM L-glutamine, 100 U/ml penicillin, 100 μg/ml streptomycin, 20 μM fluorodeoxyuridine, 20 μM uridine, and 3.3 μg/ml aphidicolin. AM50 medium consisted of AM0 medium plus 50 ng/ml mouse 2.5S NGF (Harlan Bioproducts, Indianapolis, IN). Because serum attenuates the bioactivity of CEP-1347 (Maroney et al., 1999), experiments with CEP-1347 were performed by using a modified N2 medium consisting of DMEM/F12, 40 nM progesterone, 30 nM sodium selenite, 100 μM putrescine, and 10 μg/ml transferrin (Jackson ImmunoResearch, West Grove, PA), unless indicated otherwise. The concentrations of CEP-1347 used in serum-free or serum-containing medium were 400 nM and 1.3 μM, respectively. For cerebellar granule neurons, three different media were used: K5 − S (Basal Medium Eagle's [Life Technologies] containing 5 mM KCl, 100 U/ml penicillin, and 100 μg/ml streptomycin), K5 + S (K5 − S plus 10% dialyzed fetal bovine serum), and K25 + S (K5 + S plus 20 mM KCl). The breeding and genotyping of $Bax^{-/-}$, $Bid^{-/-}$, and $Bim^{-/-}$ mice has been described previously (Knudson et al., 1995; Bouillet et al., 1999).

Sympathetic Neuronal Cultures

Primary cultures of sympathetic neurons were established from the superior cervical ganglia (SCG) of neonatal mice or rats by using previously described methods (Johnson and Argiro, 1983; Deckwerth et al., 1996). Neurons were grown in AM50 for ∼5 days in vitro (DIV) and then either maintained in AM50 or treated as follows. For NGF deprivation, cultures were rinsed with AM0, followed by the addition of AM0 containing goat anti-mouse 2.5 S NGF neutralizing antiserum (anti-NGF). For NGF deprivation in the presence of BAF, 50 μM BAF was added to AM0 containing anti-NGF.

Cerebellar Granule Neuron Cultures

Primary cultures of CGNs were obtained as described previously (Miller and Johnson, 1996). In brief, postnatal day 7 (P7) cerebella were dissected, trypsinized, triturated, and plated into K25 + S medium at a density of 2.3×10^5 cells/cm² in four-well dishes (Nunc) coated with 0.1 mg/ml poly-L-lysine. To reduce the number of nonneuronal cells, 3.3 μg/ml aphidicolin was added to the medium 36 hr after plating. At DIV5, CGNs were transfected as previously described (Moulder et al., 1999). In some experiments, cells at DIV7 were either maintained in K25 + S or switched to K5 − S (rat) or K5 + S (mouse) after washing once with the respective medium. Cell survival was assessed by a naïve observer counting the number of GFP-positive cells as described previously (Miller et al., 1997a). Because of the low transfection efficiency (∼0.1%) of these cells, expression of exogenous proteins can only be assessed by immunocytochemistry, which is not quantitative. Moreover, since all *Bim* constructs (i.e., wt and mutants) were subcloned into the same parental vector (i.e., *pEF pGKhygro* from A. Strasser), expression levels should be comparable. Accordingly, for the various *Bim* mutants described herein, immunocytochemistry for the EE epitope tag demonstrated approximately equivalent expression levels (data not shown). Finally, like previously published results (Mota et al.,

---

(F) DIV5 CGNs from $Bax^{+/+}$ or $Bax^{-/-}$ mice were cotransfected with EGFP and the indicated vector. The number of GFP-positive cells was counted 48 hr later and expressed as a percentage of vector (pcDNA3.1)-transfected cells. Mean ± SD, n = 3–4 from two independent experiments (*p ≤ 0.001, $Bax^{+/+}$ versus $Bax^{-/-}$).

2001; Whitfield et al., 2001; Xu et al., 2001), overexpression of *Bim* or kinases of the MLK/JNK pathway in CGNs caused cytochrome *c* release and caspase activation (by immunocytochemistry), as well as nuclear condensation and fragmentation (by Hoechst staining), consistent with induction of an apoptotic cell death (data not shown).

Subcellular Fractionation, Alkali Extraction, Immunoprecipitation, and Immunoblotting

Fractionation, extraction, and immunoblotting of sympathetic neurons were performed as described previously (Putcha et al., 2000). Immunoprecipitation of endogenous BIM from SCG neurons was performed as described previously (Deverman et al., 2002), with anti-BIM (Ab-1) from Oncogene Research Products. Primary antibodies for immunoblotting included α-tubulin (Sigma), Bax (Upstate), BCL-X$_L$ (H-9; Santa Cruz), Bim/Bod (StressGen), cytochrome oxidase subunit IV (COX4) (Molecular Probes), lactate dehydrogenase (LDH) (Rockland Immunochemicals), LC8 (a kind gift from S. King), JIP-3 (E-18; Santa Cruz), MKK4 (D-19; Santa Cruz), MLK3 (C-20; Santa Cruz), phospho-c-Jun S63 (P-Jun) (Cell Signaling Technologies), and phospho-Akt S473 (P-Akt) (CST). Appropriate horseradish peroxidase-conjugated secondary antibodies (CST and Jackson ImmunoResearch) were diluted 1:5000–1:10,000.

In Vitro Kinase Assay

As described previously (Le et al., 2001), different kinases, including MKK4 (0.2 μg), MKK7α (0.9 μg), JNK1α1 (0.6 μg), JNK2α2 (0.3 μg), JNK3 (0.3 μg), MLK1 (0.04 μg), MLK2 (0.1 μg), and MLK3 (0.1 μg), were incubated with buffer (control), 1 μg of wild-type GST- BIM$_{EL}$ or mutant GST- BIM$_{EL}$ proteins, and [^{32}P]ATP in kinase buffer (20 mM HEPES [pH 7.6], 20 mM MgCl$_2$, 2 mM dithiothreitol, 1 μM ATP, 0.2 mM sodium vanadate, and 25 mM β-glycerol phosphate) at 30°C for 30 min. The reactions were stopped by adding sample buffer and heating at 80°C for 10 min. The samples were loaded on 7.5% SDS-PAGE gels, dried, and analyzed on the STORM PhosphorImager system (Molecular Dynamics).

Confocal Microscopy

As described previously (Frank et al., 2001), COS-7 green monkey renal epithelial cells were grown in 4.2 cm^2 chamber slides (Nalge Nunc, Naperville, IL) and transfected using FuGENE6 transfection reagent (Roche Diagnostics, GmbH, Mannheim, Germany) according to the manufacturer's instructions. Sixteen hours after transfection and at least 30 min before treatment with 1.2 μM STS, 25 μM zVAD-fmk and 20 ng/mL MitoTracker red CMXRos (Molecular Probes) were added. Images were collected using an Olympus Fluoview confocal microscope (FV300-IX70), and RGB images were processed after acquisition by using Fluoview and Photoshop software.

Plasmids

Bim$_{EL}$, *Bim$_L$*, and *Bim$_S$* were kindly provided by A. Strasser (O'Connor et al., 1998). Wild-type and kinase-inactive forms of *Mlk2*, *Mlk3*, *Mkk4*, *Mkk7*, and *Jnk1* have been described previously (Xu et al., 2001), as has *tBid-GFP* (Nechustan et al., 2001). Site-directed mutagenesis was performed at Cytomyx (Cambridge, UK). For confocal studies, *Bim$_{EL}$* wt, *3A*, and *3E* were subcloned into *EYFP-C1* (Clonetech). The parental vector for all *Bim* constructs was *pEF pGKhygro*, whereas that for all *Mlk2*, *Mlk3*, *Mkk4*, *Mkk7*, and *Jnk1* constructs was *pcDNA3.1*.

Statistics

When indicated, statistical significance was determined by a Student's t test or by a Mann-Whitney rank sum test for parametric and nonparametric data, respectively.

References

Bennett, B.L., Sasaki, D.T., Murray, B.W., O'Leary, E.C., Sakata, S.T., Xu, W., Leisten, J.C., Motiwala, A., Pierce, S., Satoh, Y., et al. (2001). SP600125, an anthrapyrazolone inhibitor of Jun N-terminal kinase. Proc. Natl. Acad. Sci. USA *98*, 13681–13686.

Bouillet, P., Metcalf, D., Huang, D.C., Tarlinton, D.M., Kay, T.W., Kontgen, F., Adams, J.M., and Strasser, A. (1999). Proapoptotic BCL-2 relative BIM required for certain apoptotic responses, leukocyte homeostasis, and to preclude autoimmunity. Science *286*, 1735–1738.

Bouillet, P., Zhang, L.C., Huang, D.C., Webb, G.C., Bottema, C.D., Shore, P., Eyre, H.J., Sutherland, G.R., and Adams, J.M. (2001). Gene structure, alternative splicing, and chromosomal localization of pro-apoptotic BCL-2 relative BIM. Mamm. Genome *12*, 163–168.

Coffey, E.T., Hongisto, V., Dickens, M., Davis, R.J., and Courtney, M.J. (2000). Dual roles for c-Jun N-terminal kinase in developmental and stress responses in cerebellar granule neurons. J. Neurosci. *20*, 7602–7613.

Coffey, E.T., Smiciene, G., Hongisto, V., Cao, J., Brecht, S., Herdegen, T., and Courtney, M.J. (2002). c-Jun N-terminal protein kinase (JNK) 2/3 is specifically activated by stress, mediating c-Jun activation, in the presence of constitutive JNK1 activity in cerebellar neurons. J. Neurosci. *22*, 4335–4345.

Crowder, R.J., and Freeman, R.S. (1999). The survival of sympathetic neurons promoted by potassium depolarization, but not by cyclic AMP, requires phosphatidylinositol 3-kinase and Akt. J. Neurochem. *73*, 466–475.

Deckwerth, T.L., Elliott, J.L., Knudson, C.M., Johnson, E.M., Snider, W.D., and Korsmeyer, S.J. (1996). BAX is required for neuronal death after trophic factor deprivation and during development. Neuron *17*, 401–411.

Deverman, B.E., Cook, B.L., Manson, S.R., Niederhoff, R.A., Langer, E.M., Rosova, I., Kulans, L.A., Fu, X., Weinberg, J.S., Heinecke, J.W., et al. (2002). BCL-X$_L$ deamidation is a critical switch in the regulation of the response to DNA damage. Cell *111*, 51–62.

Dijkers, P.F., Medema, R.H., Lammers, J.W., Koenderman, L., and Coffer, P.J. (2000). Expression of the pro-apoptotic BCL-2 family member BIM is regulated by the forkhead transcription factor FKHR-L1. Curr. Biol. *10*, 1201–1204.

Dijkers, P.F., Birkenkamp, K.U., Lam, E.W., Thomas, N.S., Lammers, J.W., Koenderman, L., and Coffer, P.J. (2002). FKHR-L1 can act as a critical effector of cell death induced by cytokine withdrawal: protein kinase B-enhanced cell survival through maintenance of mitochondrial integrity. J. Cell Biol. *156*, 531–542.

Dudek, H., Datta, S.R., Franke, T.F., Birnbaum, M.J., Yao, R., Cooper, G.M., Segal, R.A., Kaplan, D.R., and Greenberg, M.E. (1997). Regulation of neuronal survival by the serine-threonine protein kinase Akt. Science *275*, 661–665.

Eilers, A., Whitfield, J., Babij, C., Rubin, L.L., and Ham, J. (1998). Role of the Jun kinase pathway in the regulation of c-Jun expression and apoptosis in sympathetic neurons. J. Neurosci. *18*, 1713–1724.

Estus, S., Zaks, W.J., Freeman, R.S., Gruda, M., Bravo, R., and Johnson, E.M., Jr. (1994). Altered gene expression in neurons during programmed cell death: identification of c-jun as necessary for neuronal apoptosis. J. Cell Biol. *127*, 1717–1727.

Frank, S., Gaume, B., Bergmann-Leitner, E.S., Leitner, W.W., Robert, E.G., Catez, F., Smith, C.L., and Youle, R.J. (2001). The role of dynamin-related protein *1*, a mediator of mitochondrial fission, in apoptosis. Dev. Cell *1*, 515–525.

Haase, M., Koslowski, R., Lengnick, A., Hahn, R., Wenzel, K.W., Schuh, D., Kasper, M., and Muller, M. (1997). Cellular distribution of c-Jun and c-Fos in rat lung before and after bleomycin induced injury. Virchows Arch. *431*, 441–448.

Ham, J., Babij, C., Whitfield, J., Pfarr, C.M., Lallemand, D., Yaniv, M., and Rubin, L.L. (1995). A c-Jun dominant negative mutant protects sympathetic neurons against programmed cell death. Neuron *14*, 927–939.

Han, Z., Boyle, D.L., Chang, L., Bennett, B., Karin, M., Yang, L., Manning, A.M., and Firestein, G.S. (2001). c-Jun N-terminal kinase is required for metalloproteinase expression and joint destruction in inflammatory arthritis. J. Clin. Invest. *108*, 73–81.

Harris, C.A., and Johnson, E.M., Jr. (2001). BH3-only BCL-2 family members are coordinately regulated by the JNK pathway and require BAX to induce apoptosis in neurons. J. Biol. Chem. *276*, 37754–37760.

Harris, C.A., Deshmukh, M., Tsui-Pierchala, B., Maroney, A.C., and Johnson, E.M., Jr. (2002a). Inhibition of the c-Jun N-terminal kinase signaling pathway by the mixed lineage kinase inhibitor CEP-1347 (KT7515) preserves metabolism and growth of trophic factor-deprived neurons. J. Neurosci. *22*, 103–113.

Harris, C.A., Maroney, A.C., and Johnson, E.M., Jr. (2002b). Identification of JNK-dependent and independent components of cerebellar granule neuron apoptosis. J. Neurochem. *83*, 992–1001.

Imaizumi, K., Tsuda, M., Imai, Y., Wanaka, A., Takagi, T., and Tohyama, M. (1997). Molecular cloning of a novel polypeptide, Dp5, induced during programmed neuronal death. J. Biol. Chem. *272*, 18842–18848.

Johnson, M.I., and Argiro, V. (1983). Techniques in the tissue culture of rat sympathetic neurons. Methods Enzymol. *103*, 334–347.

Khokhlatchev, A.V., Canagarajah, B., Robinson, M., Atkinson, M., Goldsmith, E., and Cobb, M.H. (1998). Phosphorylation of the MAP kinase ERK2 promotes its homodimerization and nuclear translocation. Cell *93*, 605–615.

Knudson, C.M., Tung, K.S., Tourtellotte, W.G., Brown, G.A., and Korsmeyer, S.J. (1995). Bax-deficient mice with lymphoid hyperplasia and male germ cell death. Science *270*, 96–99.

Le, S., Connors, T.J., and Maroney, A.C. (2001). c-Jun N-terminal kinase specifically phosphorylates p66ShcA at serine 36 in response to ultraviolet irradiation. J. Biol. Chem. *276*, 48332–48336.

LeBlanc, H., Lawrence, D., Varfolomeev, E., Totpal, K., Morlan, J., Schow, P., Fong, S., Schwall, R., Sinicropi, D., and Ashkenazi, A. (2002). Tumor-cell resistance to death receptor–induced apoptosis through mutational inactivation of the proapoptotic BCL-2 homolog BAX. Nat. Med. *8*, 274–281.

Lei, K., Nimnual, A., Zong, W.X., Kennedy, N.J., Flavell, R.A., Thompson, C.B., Bar-Sagi, D., and Davis, R.J. (2002). The Bax subfamily of Bcl2-related proteins is essential for apoptotic signal transduction by c-Jun NH(2)-terminal kinase. Mol. Cell. Biol. *22*, 4929–4942.

Li, H., Kolluri, S.K., Gu, J., Dawson, M.I., Cao, X., Hobbs, P.D., Lin, B., Chen, G., Lu, J., Lin, F., et al. (2000). Cytochrome c release and apoptosis induced by mitochondrial targeting of nuclear orphan receptor TR3. Science *289*, 1159–1164.

Lindsten, T., Ross, A.J., King, A., Zong, W., Rathmell, J.C., Shiels, H.A., Ulrich, E., Waymire, K.G., Mahar, P., Frauwirth, K., et al. (2000). The combined functions of proapoptotic BCL-2 family members BAK and BAX are essential for normal development of multiple tissues. Mol. Cell *6*, 1389–1399.

Liu, D.X., and Greene, L.A. (2001). Regulation of neuronal survival and death by E2F-dependent gene repression and derepression. Neuron *32*, 425–438.

Maroney, A.C., Finn, J.P., Bozyczko-Coyne, D., O'Kane, T.M., Neff, N.T., Tolkovsky, A.M., Park, D.S., Yan, C.Y., Troy, C.M., and Greene, L.A. (1999). CEP-1347 (KT7515), an inhibitor of JNK activation, rescues sympathetic neurons and neuronally differentiated PC12 cells from death evoked by three distinct insults. J. Neurochem. *73*, 1901–1912.

Maroney, A.C., Finn, J.P., Connors, T.J., Durkin, J.T., Angeles, T., Gessner, G., Xu, Z., Meyer, S.L., Savage, M.J., Greene, L.A., et al.

(2001). CEP-1347 (KT7515), a semisynthetic inhibitor of the mixed lineage kinase family. J. Biol. Chem. *276*, 25302–25308.

Miller, T.M., and Johnson, E.M., Jr. (1996). Metabolic and genetic analyses of apoptosis in potassium/serum-deprived rat cerebellar granule cells. J. Neurosci. *16*, 7487–7495.

Miller, T.M., Moulder, K.L., Knudson, C.M., Creedon, D.J., Deshmukh, M., Korsmeyer, S.J., and Johnson, E.M., Jr. (1997a). Bax deletion further orders the cell death pathway in cerebellar granule cells and suggests a caspase-independent pathway to cell death. J. Cell Biol. *139*, 205–217.

Miller, T.M., Tansey, M.G., Johnson, E.M., Jr., and Creedon, D.J. (1997b). Inhibition of phosphatidylinositol 3-kinase activity blocks depolarization- and insulin-like growth factor I-mediated survival of cerebellar granule cells. J. Biol. Chem. *272*, 9847–9853.

Mota, M., Reeder, M., Chernoff, J., and Bazenet, C.E. (2001). Evidence for a role of mixed lineage kinases in neuronal apoptosis. J. Neurosci. *21*, 4949–4957.

Moulder, K.L., Onodera, O., Burke, J.R., Strittmatter, W.J., and Johnson, E.M., Jr. (1999). Generation of neuronal intranuclear inclusions by polyglutamine-GFP: analysis of inclusion clearance and toxicity as a function of polyglutamine length. J. Neurosci. *19*, 705–715.

Nechustan, A., Smith, C.L., Lamensdorf, I., Yoon, S.H., and Youle, R.J. (2001). BAX and BAK coalesce into novel mitochondria-associated clusters during apoptosis. J. Cell Biol. *153*, 1265–1276.

O'Connor, L., Strasser, A., O'Reilly, L.A., Hausmann, G., Adams, J.M., Cory, S., and Huang, D.C. (1998). BIM: A novel member of the BCL-2 family that promotes apoptosis. EMBO J. *17*, 384–395.

Ogita, K., Okuda, H., Kitano, M., Fujinami, Y., Ozaki, K., and Yoneda, Y. (2002). Localization of activator protein-1 complex with DNA binding activity in mitochondria of murine brain after in vivo treatment with kainate. J. Neurosci. *22*, 2561–2570.

Putcha, G.V., Deshmukh, M., and Johnson, E.M., Jr. (2000). Inhibition of apoptotic signaling cascades causes loss of trophic factor dependence during neuronal maturation. J. Cell Biol. *149*, 1011–1018.

Putcha, G.V., Moulder, K.L., Golden, J.P., Bouillet, P., Adams, J.A., Strasser, A., and Johnson, E.M. (2001). Induction of BIM, a proapoptotic BH3-only BCL-2 family member, is critical for neuronal apoptosis. Neuron *29*, 615–628.

Putcha, G.V., Harris, C.A., Moulder, K.L., Easton, R.M., Thompson, C.B., and Johnson, E.M., Jr. (2002). Intrinsic and extrinsic pathway signaling during neuronal apoptosis: lessons from the analysis of mutant mice. J. Cell Biol. *157*, 441–453.

Puthalakath, H., Huang, D.C., O'Reilly, L.A., King, S.M., and Strasser, A. (1999). The proapoptotic activity of the Bcl-2 family member Bim is regulated by interaction with the dynein motor complex. Mol. Cell *3*, 287–296.

Shinjyo, T., Kuribara, R., Inukai, T., Hosoi, H., Kinoshita, T., Miyajima, A., Houghton, P.J., Look, A.T., Ozawa, K., and Inaba, T. (2001). Downregulation of BIM, a proapoptotic relative of BCL-2, is a pivotal step in cytokine-initiated survival signaling in murine hematopoietic progenitors. Mol. Cell. Biol. *21*, 854–864.

Tournier, C., Hess, P., Yang, D.D., Xu, J., Turner, T.K., Nimnual, A., Bar-Sagi, D., Jones, S.N., Flavell, R.A., and Davis, R.J. (2000). Requirement of JNK for stress-induced activation of the cytochrome c-mediated death pathway. Science *288*, 870–874.

Trotter, L., Panton, W., Hajimohamadreza, I., Petalidis, L., Ward, R., Fleming, Y., Armstrong, C.G., Cohen, P., Karran, E.H., and Kinloch, R.A. (2002). Mitogen-activated protein kinase kinase 7 is activated during low potassium-induced apoptosis in rat cerebellar granule neurons. Neurosci. Lett. *320*, 29–32.

Vaillant, A.R., Mazzoni, I., Tudan, C., Boudreau, M., Kaplan, D.R., and Miller, F.D. (1999). Depolarization and neurotrophins converge on the phosphatidylinositol 3-kinase-Akt pathway to synergistically regulate neuronal survival. J. Cell Biol. *146*, 955–966.

Wei, M.C., Zong, W.X., Cheng, E.H., Lindsten, T., Panoutsakopoulou, V., Ross, A.J., Roth, K.A., MacGregor, G.R., Thompson, C.B., and Korsmeyer, S.J. (2001). Proapoptotic BAX and BAK: A requisite gateway to mitochondrial dysfunction and death. Science *292*, 727–730.

Whitfield, J., Neame, S.J., Paquet, L., Bernard, O., and Ham, J. (2001). Dominant-negative c-Jun promotes neuronal survival by reducing BIM expression and inhibiting mitochondrial cytochrome *c* release. Neuron *29*, 629–643.

Xu, X., Raber, J., Yang, D., Su, B., and Mucke, L. (1997). Dynamic regulation of c-Jun N-terminal kinase activity in mouse brain by environmental stimuli. Proc. Natl. Acad. Sci. USA *94*, 12655–12660.

Xu, Z., Maroney, A.C., Dobrzanski, P., Kukekov, N.V., and Greene, L.A. (2001). The MLK family mediates c-Jun N-terminal kinase activation in neuronal apoptosis. Mol. Cell. Biol. *21*, 4713–4724.

Zong, W.X., Lindsten, T., Ross, A.J., MacGregor, G.R., and Thompson, C.B. (2001). BH3-only proteins that bind pro-survival BCL-2 family members fail to induce apoptosis in the absence of BAX and BAK. Genes Dev. *15*, 1481–1486.